Content-Aware Transmission in UAV-Assisted Multicast Communication

Mingze Zhang, *Student Member, IEEE,* Yifeng Xiong, *Student Member, IEEE,*
Soon Xin Ng, *Senior Member, IEEE* and Mohammed El-Hajjar, *Senior Member, IEEE,*

***Abstract*—To alleviate the explosive growth of data traffic caused by the increased use of smart devices, new transmission techniques are needed to increase the utilization of limited bandwidth resources and for providing high transmission rates in future wireless networks. On the other hand, due to their flexibility and autonomy, unmanned aerial vehicles (UAVs) are considered as a potential candidate to support ubiquitous connectivity and operate as flying base stations, where the deployment of UAVs can affect the quality of experience (QoE) of users. Hence, in this paper, we employ UAVs as aerial base stations to transmit data to ground users (GUs) via air to ground (A2G) communication links, where we show how content awareness can help improve the data rate. Specifically, we design two content-sharing (CS) data transmission schemes to improve the average data rate of the GUs. Additionally, two UAV deployment strategies, namely the fixed-point deployment scheme and traverse-search deployment scheme, are proposed based on the proposed CS transmission schemes. The simulation results demonstrate that our proposed data transmission schemes combined with their proposed deployment schemes outperform the traditional transmission scheme by 26 bits/s/Hz and 51 bits/s/Hz, respectively.**

***Index Terms*—UAV, content-aware, OFDMA, aerial base station, resource allocation, deployment.**

I. Introduction

NOWADAYS, the development of wireless communication technologies and the termination techniques has trigged the explosive increasement of mobile data traffic [1]. The increasing mobile data traffic is mainly caused by the emerging applications of mobile devices, such as the Internet of Things, Internet of Vehicles and virtual/augmented reality, which heavily rely on high data rate and low-latency transmission [2]. However, the aforementioned applications bring new challenges to the existing mobile networks. To meet the unprecedented traffic demand and to overcome the challenges, the computing and the caching capabilities at the edge of networks are considered as a promising solution to yield significant gains for both users and operators [3], [4]. The idea of caching was first introduced in computer systems for describing a memory with small capacity but with fast access requirement. Then, this idea was applied to the Internet for retrieving a webpage from small servers instead of a central server or core network, which helps to reduce the bandwidth usage and the access time [5]. Afterwards, the idea of caching was considered in wireless communication networks to improve the content delivery process [6]. In cache-enabled wireless networks, the popular contents are usually fetched from the core network during off-peak times [7], [8], and the users can directly receive the requested contents from the edge nodes rather than from the core network. As a result, the transmission latency can be significantly reduced since the data is closer to the users.

Meanwhile, unmanned aerial vehicles (UAVs) have been receiving high attention for their mobility, manoeuvrability, and broad range of application domains in future wireless communication networks [9], [10]. The UAVs are capable of flying freely and they can either be autonomous or controlled by ground stations [11]. The application of these UAVs offers promising new ways to accomplish civilian and military missions [12], [13]. It can be found that UAV-assisted applications, which support ground users (GUs), existing terrestrial infrastructures and communication entities, are experiencing a significant increase in research interests [14]. In cellular networks, UAVs have been adopted as aerial base stations (BSs) to offload data from conventional BSs during events [15], [16] or to provide rapid and emergency wireless communication service in disaster struck areas, for example, [17] and [18]. On the other hand, UAVs can also function as flying user equipments, which is known as cellular-connected UAVs, in coexistence with GUs [19]. More specially, the main motivation of deploying UAVs as aerial BSs is due to their ability to adjust their altitude, avoid obstacles, and enhance the likelihood of line of sight (LoS) communication links to GUs [20]. Additionally, the cellular-connected UAV is a cost-effective solution since building new cellular infrastructures is expensive. Therefore, deploying UAVs as aerial BSs has many opportunities to explore in the future. Besides, UAVs are capable of serving as edge network controllers for their onboard computing abilities and storage resources [21]. Consequently, popular contents can be closer to end users by utilizing the storage resources at the edge nodes [22]. Therefore, to further alleviate the pressure of cellular networks and reduce the cost of densely deployed terrestrial BSs, caching capability can be deployed at the UAVs [23].

Additionally, by exploiting the property of contents reuse, multicast communication becomes one of the promising solutions for the explosively growing content-centric applications [24]. The authors of [25] proposed a content-aware and energy-efficient resource allocation scheme for multi-user orthogonal frequency-division multiplexing (OFDM) systems based on the perceptual quality aspects of the transmitted video. In [26], a content-aware cooperative transmission strat-

The authors are with the School of Electronics and Computer Science, University of Southampton, Southampton SO17 1BJ, United Kingdom (email:{mz6u17,yx8n18,sxn,meh}@ecs.soton.ac.uk).

egy was proposed to improve the transmission data rate by offloading users from macro BSs to small BSs. Besides, a content and computation-aware communication control framework was proposed in [27] based on the software defined network paradigm to realise an adaptable and programmable user-controlled platform. Moreover, the authors of [28] jointly optimized the locations and beamforming for cooperative content-aware UAVs to maximize the user admission. Furthermore, the authors of [28] extended the work by considering the limited storage capacity on UAVs to meet the demand of minimum rate required by users in [29]. In addition, the works of [30] developed a fountain-coding aided secure image transmission approach by considering delay and content awareness. Subsequently, a reinforcement learning based content-aware resource allocation scheme was proposed in [31] to meet users' requested data rate.

Furthermore, a multiple access scheme based on the concept of rate splitting (RS) and linear precoding, referred to as rate splitting multiple access (RSMA), has been investigated in [32], [33]. The concept of RS has been studied in [34], where the authors developed a transmission scheme that divide its message into private and common parts in a two-user scenario, which can achieve the boundary of the capacity region with optimal power and rate allocation policies. Afterwards, the authors of [35] extended the idea of RS into multi-user scenario by considering multi-input multi-output (MIMO) and multi-input single-output (MISO). Recently, the RS has now been extended to RSMA that combines space-division multiple access and non-orthogonal multiple access by linear precoding to flexibly manage interference [36]. However, before the existence of RSMA, the most widely used multiple access techniques is orthogonal frequency-division multiple access (OFDMA) [37]–[39], which is widely used in today's wireless communication systems. The main advantage of OFDMA when compared with OFDM is that it has a more flexible utilization of subcarriers, which allows multiple access to the air interface at the same time [37].

On the other hand, compared to the traditional terrestrial counterparts that have stable power supply from the power grid, a number of technical challenges, such as deployment and resource allocation, need to be addressed before integrating UAVs to the existing cellular networks. Several recent studies have been carried out to design UAV deployment strategies, where a constrained k-means clustering based real-time deployment in disaster communication was proposed in [40]. Besides, the authors of [17] jointly considered the optimization of UAV deployment and resource allocation by fast k-means algorithm for disaster relief. The authors of [41] proposed a 3-dimensional deployment scheme for supporting all GUs in multi-UAV communication frameworks, which aims for throughput maximization in the presence of co-channel interference. In [42], an adaptive UAV deployment scheme is proposed to solve the coverage problem of UAV-assisted communication system, which aims to optimize the location of the UAV to cover as many GUs as possible and reduce communication energy consumption. Subsquently, a two-layer joint optimization method was proposed in [43] in order to minimize the average task response time by by jointly optimizing UAV deployment and computation offloading. In addition, the authors of [44] proposed an improved mean shift algorithm, which jointly optimizing the location and number of UAV edge servers, to optimize the total energy consumption and deployment cost of UAVs. Furthermore, the authors of [45] proposed an effective multi-agent collaborative environment learning algorithm to realize the dynamic resource allocation of UAV networks to optimize the coverage and utility.

Compared to those previous works, we utilize the concept of content awareness to improve the average data rate of GUs in a cache-enabled UAV-assisted wireless communication system and we develop two UAV deployment schemes based on our proposed transmission schemes. Hence, given the above background, we propose to use UAV as aerial BS to increase the probability of having LoS communication links. Meanwhile, we employ OFDMA based techniques to support multiple GUs simultaneously, where content awareness can help to effectively utilize the limited bandwidth resources in our UAV-assisted wireless communication system. This allows to increase the average data rate by sharing the contents among GUs. However, it is worth noting that GUs can only fetch contents from those accessible subcarriers that include the contents they need. Accordingly, we propose two content-sharing (CS) schemes, the private content-sharing (PCS) and the common content-sharing (CCS) schemes, to improve the utilization of bandwidth resources by sharing the contents requested by GUs. Furthermore, the deployment of UAVs will also affect the transmission rates of the GUs. Therefore, we develop a fixed-point iteration based deployment scheme for PCS and a traverse-search deployment scheme for CCS to further improve the average rate of GUs in the target area [46]. Ultimately, our contributions can be summarized as follows:

1) In this work, we design a new data transmission scheme refered to as CS in a content-aware scenario to effectively utilize the limited bandwidth resources of UAVs by sharing different components of each content, where the different components of each content carried by different subcarriers are not dedicated to one specific GU and can be obtained by more GUs if accessible and needed.
2) Moreover, this allows more flexibility in the allocation of contents in these subcarriers. To further exploit the utilization of bandwidth resources of the UAVs, we propose an improved CS method, where the information each subcarrier can carry is expected to be a mixture of contents' components. Therefore, the average rate of GUs can be further improved by optimizing the weight of each content in each subcarrier.
3) Additionally, a fixed-point iteration based deployment scheme is proposed for deploying the UAV in our proposed PCS transmission scheme. However, considering that the sum weight is different at different locations for the CCS method, a traverse-search based deployment is employed to accomplish the task of UAV deployment.
4) Finally, we shows that the UAV is capable of finding the appropriate position to deploy itself according to the location of GUs in a short time. Moreover, the

proposed transmission scheme significantly increases the SE to about four times of that in traditional OFDMA communication system.

The rest of this paper is organized as follows. In Section II, we present the transmission model of our proposed UAV-assisted communication system. Then, the deployment of UAV is introduced in Section III. Afterwards, we analyze our simulation results in Section IV followed by our conclusions in Section V.

II. Transmission Model

In this paper, we consider a UAV-assisted communication system in a downlink scenario to serve a number of GUs in its target area, as shown in Fig. 1. In this case, the UAV is employed as a flying BS to establish stable and reliable air to ground (A2G) communication links to serve the GUs[1]. Besides, the UAV is equipped with caching capability[2], where the data requested by the GUs can be cached and ready for transmission to the GUs. Moreover, the UAV is capable of flying horizontally and hovering at a certain altitude of h_d and it also knows the locations of the GUs [47]. Meanwhile, OFDMA technique is employed to support the A2G communication links between the UAV and the multiple GUs. Here, the bandwith resource is divided into subcarriers, which are assigned to GUs according to their real-time requirements [48].

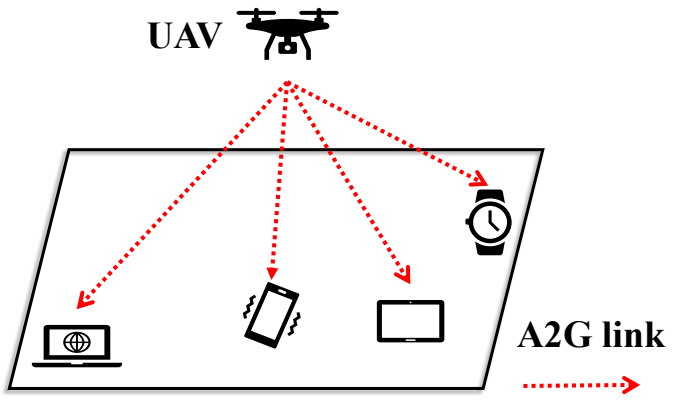

Fig. 1: UAV-assisted network model that provides service of wireless communication for GUs.

Additionally, we assume that all GUs generate their own request periodically based on their preferences, which can be represented by a set of distributions. Fig. 2 shows an example of GU's preference represented by the distribution of available contents, where a total of 50 different contents have been taken into consideration and each can be thought of as a category (e.g. sports, weather, literature.). The probability is used to measure the level of user interests in each content, where the higher the probability, the greater the chance of being requested. However, since the requested contents are all known by the UAV as a flying BS and the bandwidth resources on the UAV is limited, it is necessary to design new transmission schemes to fully utilize the limited bandwidth resources. Besides, the UAV's deployment location also needs to be adjusted to further improve the downlink performance by exploiting the flexibility and maneuverability of the UAV.

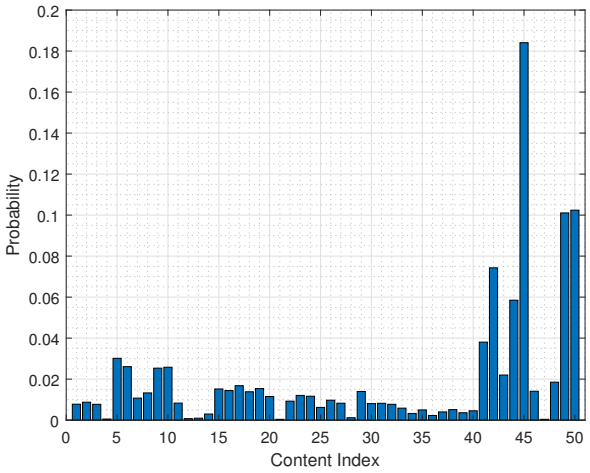

Fig. 2: An example of GU preference represented by content distribution.

Moreover, we assume that all GUs are capable of achieving their maximum achievable rate on their assigned subcarrier in an OFDMA system. For simplicity, the whole bandwidth will be equally divided into subcarriers according to the number of GUs N_u and each GU will be assigned one subcarrier, which means the number of subcarriers $N_s = N_u$. The achievable rate is only related to the received signal power P_r, when the bandwidth B and the noise power spectral density (PSD) N_0 are fixed. Besides, due to the dynamic A2G distances of the GUs, the different GUs will receive the OFDM modulated signal with different received signal power. Therefore, the achiveable rate of each subcarrier is different for different GUs. For example, consider a system supporting two GUs and each is assigned with one subcarrier, where the received signal power of the first GU is assumed stronger than that of the second GU ($P_r^1 > P_r^2$). In this case, the data throughput that the first GU can be supported based on its assigned subcarrier is higher than that of the second GU. Additionally, we consider the case that each subcarrier is modulated depending on the received signal power of its assigned GU. Hence, the first GU is capable of correctly recovering the information on both subcarriers while the second GU can only recover the information of its own subcarrier. This is because the power needed to demodulate the information of the first subcarrier, which is also the first GU's subcarrier, should be greater than or equal to P_r^1, while the second GU has a lower received power.

In our system, subcarriers are preallocated to GUs before the transmission and the information is encoded based on the channel condition of the GUs. Accordingly, it can be found that one GU can only demodulate the subcarriers that have a reduced received power in our proposed communication

[1] The case illustrated here is one UAV with its associated GUs. However, the scheme can also be applied to a scenario of multiple UAVs and each UAV has their own associated GUs.

[2] The store of contents may cause additional power usage and affect the battery life of the UAV, which will be investigated in our future work.

system. In the following, we will present the channel model of the proposed UAV-assisted communication followed by the structure of our proposed CS-OFDMA. Afterwards, two CS schemes, namely PCS and CCS, will be detailed.

A. Channel model

Since the UAV is operating as an aerial BS to serve the GUs at a certain height h_d in our system, the communication links between the GUs and the UAV can be considered to be in strong LoS propagation environment [49]. Therefore, the Rician fading channel model [50], which is composed of a dominant LoS path and some non line of sight (NLoS) paths, is considered to model the signal propagation environment [51]. The Rician channel employed in our A2G communication decomposes the channel into two components [52]: deterministic LoS component h_{LoS} and stochastic NLoS component h_{NLoS}. Then, the channel h is given by:

$$h = \sqrt{\frac{K}{1+K}} \cdot h_{\text{LoS}} + \sqrt{\frac{1}{1+K}} \cdot h_{\text{NLoS}}, \tag{1}$$

where h_{NLoS} is used to describe the scattered multipath propagation of signals, while the Rician K factor is the power ratio of the LoS path and the NLoS paths. Accordingly, the Rician K factor in our UAV-assisted communication system ranges from 0.51 to 6.31 [53], to generate a LoS dominant channel.

On the other hand, path loss is commonly considered to measure the signal attenuation in A2G communication system. Path loss is closely linked with the environment, where the transmitter and receiver are operating [54]. Generally, the propagation path loss P_l can be expressed by [55]:

$$P_l = \left(\frac{4\pi}{\lambda}\right)^2 d^{\alpha}, \tag{2}$$

where d indicates the distance between the transmitter and receiver, while the path loss exponent α, which ranges from 2 to 6, indicates the nature of the propagation environment. The wavelength $\lambda = \frac{c}{f_c}$ is defined as the ratio of the speed of light c in m/s to the carrier frequency f_c in Hz. Therefore, the received signal power P_r given a transmission power P_t is formulated as [56]:

$$P_r = \frac{P_t}{P_l} = P_t \left(\frac{c}{4\pi f_c}\right)^2 \left(\frac{1}{d}\right)^{\alpha}. \tag{3}$$

In our UAV-assisted communication system, the UAV is considered to fly at a given altitude of $h_d = 100$ m [57] and the LoS communication links are assumed to exist for most of the time [49]. Under the LoS model, the free space path loss exponent $\alpha = 2$ is chosen to describe the signal attenuation. Then, the received signal power P_r can be represented as:

$$P_r = P_t \left(\frac{c}{4\pi d f_c}\right)^2. \tag{4}$$

Additionally, one important criterion to measure the performance of a system is the achievable rate and the channel capacity C in bits per second (bits/s) that uses the received signal power P_r perturbed by additive white Gaussian noise (AWGN) of PSD N_0 with bandwidth B is given by [58]:

$$C = B \log_2 \left(1 + \frac{P_r}{B N_0}\right). \tag{5}$$

B. Proposed content-sharing based transmission

In this work, we consider a UAV-assisted communication system for supporting GUs, where content awareness can be utilized to improve the average data rate. Accordingly, it can be seen that two parameters, the power allocation coefficient and the composition of content, can be optimized to improve the utilization of the limited bandwidth resources, which is similar to the concept of RS. Therefore, inspired by the concept of RS that splits the message into common and private parts, we apply the RS concept to traditional OFDMA modulation in order to improve the throughput due to the fact that a common part will be shared by multiple users, which would largely increase the bandwidth utilization. Moreover, we assume that all contents cannot be transmitted by just one transmission, which means each OFDM frame can carry only parts of those requested contents by preallocated subcarriers. Therefore, if three users request the same content and each user is assigned one subcarrier, then these three subcarriers carry three different parts of this content.

Fig. 3 shows the structure of the proposed CS-OFDMA system, where instead of separating the users by different power layers in RSMA, the users are partitioned by frequency (subcarriers). Then, we consider a two-layer RS structure in each subcarrier to separate the private and common messages since users are already separated by subcarriers. In each subcarrier, the private message means the content requested by the GU assigned with this subcarrier, while the common message is a mixture of all possible contents considered in this system but with different proportion. Moreover, given that $N_s = N_u$, the information to be conveyed to the i^{th} GU is carried by the i^{th} subcarrier, which means the private message carried by the i^{th} subcarrier is modulated based on h_i^i, where h_i^i is the channel gain of the i^{th} GU at the i^{th} subcarrier. Meanwhile, a threshold h_T is set to modulate the common message, which will be further explained in the following sections. Therefore, the contents conveyed by each subcarrier cannot be demodulated by all GUs, especially for the common message. Then, the contents modulated on the common part in each subcarrier need to be adjusted based on the number of GUs who can successfully demodulate the information conveyed by the specific subcarrier and the contents requested by those accessible GUs. As a result, the transmitted signal modulated on the i^{th} subcarrier can be expressed as:

$$x_i = \sqrt{p_i} x_c^i + \sqrt{1-p_i} x_p^i, \tag{6}$$

where p_i is the power allocation coefficient of the common message in the i^{th} subcarrier, subject to the constraint $0 \leq p_i \leq 1$, while x_c^i and x_p^i represent the common message and the private message of the i^{th} subcarrier, respectively. Consequently, the total received signal of the u^{th} GU at the i^{th} subcarrier is given by:

$$y_u^i = h_u^i x_i + n_i = \sqrt{p_i} h_u^i x_c^i + \sqrt{1-p_i} h_u^i x_p^i + n_i, \tag{7}$$

where h_u^i represents the channel gain including the path loss of the u^{th} GU at the i^{th} subcarrier and n_i is the AWGN with variance σ^2 at the i^{th} subcarrier. In the following, it should be noted that we will use h_i to represent h_i^i for brevity.

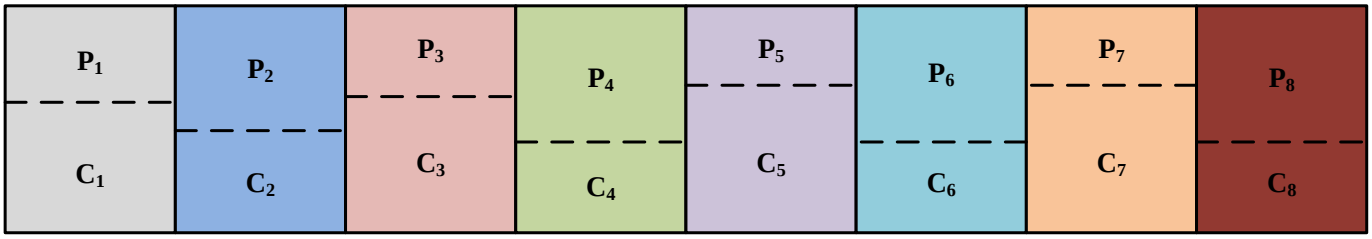

Fig. 3: A toy example of CS-OFDMA in frequency domain with RS in each subcarrier, where "P" indicates the private message and "C" indicates the common message.

As mentioned before, each GU is only allowed to demodulate those subcarriers that have weaker received signal power or weaker channel condition than its allocated subcarrier. It is worth noting that we consider the scenario where the weakest channel condition can also support the basic A2G communication. Here, the common message is public for all GUs, while the private message cannot. Besides, it can be seen that the common message in a subcarrier can be demodulated or utilized by more GUs if a weaker channel power is used to modulate the common message. In an extreme case, the system employs the weakest channel among those GUs as h_T to modulate the common message, then the common message in each subcarrier is available for all GUs. However, it is highly possible that the sum rate can be lower even though the number of GUs who can access the subcarriers is increased, because the channel condition employed is too weak to support a high-speed data transmission. As a result, a threshold h_T needs to be firstly set for the received signal power over all subcarriers before formulating the rate of the common message. In fact, the threshold is used to control the accessibility of the common message in each subcarrier and further affect the sum rate. As an example, let us consider a two-GUs scenario that has $|h_1|^2 > |h_T|^2 > |h_2|^2$. Then, only the first GU can obtain the common message on both subcarriers as well as its private message modulated on its own subcarrier, while the second GU can only obtain the private message on its assigned subcarrier since the common message of all subcarriers is modulated based on h_T.

Based on the above discussion, we know that a GU can only demodulate the subcarriers that have a poorer channel condition. Therefore, to calculate the data rate of the system, a filter vector $\boldsymbol{F}_i \in \mathbb{C}^{N_s \times 1}$ needs to be defined to demonstrate the accessibility of the i^{th} subcarrier, which is used to count the utilization of the common message. For instance, we consider a group of 6 GUs and each of them is assigned with one subcarrier. Besides, the channel gain of each GU in a descending order is represented by $|h_2|^2 < |h_3|^2 < |h_1|^2 < |h_5|^2 < |h_6|^2 < |h_4|^2$. Consequently, the filter vector of each subcarrier can be expressed by:

$$\begin{aligned} \boldsymbol{F}_1 &= [1,1,1,0,0,0]^T, \quad \boldsymbol{F}_2 = [0,1,0,0,0,0]^T, \\ \boldsymbol{F}_3 &= [0,1,1,0,0,0]^T, \quad \boldsymbol{F}_4 = [1,1,1,1,1,1]^T, \\ \boldsymbol{F}_5 &= [1,1,1,0,1,0]^T, \quad \boldsymbol{F}_6 = [1,1,1,0,1,1]^T. \end{aligned} \tag{8}$$

In $\boldsymbol{F}_1$, the power of the first subcarrier p_1 ranks third among all subcarriers, and the two that have stronger received signal power are GU_2 and GU_3. Hence, only the first three positions of $\boldsymbol{F}_1$ have been set to "1".

Meanwhile, the weight vector $\boldsymbol{W}_i \in \mathcal{W}_I = \{\boldsymbol{W}_1, \boldsymbol{W}_2, \ldots, \boldsymbol{W}_i, \ldots, \boldsymbol{W}_{N_s}\}$ is used to indicate the percentage of content in the common part of the i^{th} subcarrier, for $i = 1, 2, 3, \ldots, N_s$. $\boldsymbol{W}_i$ represents the weight vector of the i^{th} subcarrier, given by $\boldsymbol{W}_i = [w_{i1}, w_{i2}, \ldots, w_{ij}, \ldots, w_{iN_c}]$, where w_{ij} is the weight of the j^{th} content in the i^{th} subcarrier. Additionally, the weight vector $\boldsymbol{W}_i$ is also subject to the constraint $\sum_{j=1}^{N_c} w_{ij} = 1$, where $0 \leq w_{ij} \leq 1$ and N_c is the number of contents considered in the system. Afterwards, a selection matrix $\boldsymbol{S} \in \mathbb{C}^{N_c \times N_u}$ is necessary to link the N_u GUs with their corresponding contents and the selection matrix $\boldsymbol{S}$ is in the form of:

$$\boldsymbol{S} = \begin{bmatrix} s_{11} & s_{12} & \cdots & s_{1N_u} \\ s_{21} & s_{22} & \cdots & s_{2N_u} \\ \vdots & \vdots & \ddots & \vdots \\ s_{N_c1} & s_{N_c2} & \cdots & s_{N_cN_u} \end{bmatrix}, \tag{9}$$

where s_{ju} represents the flag of the j^{th} content from the u^{th} GU, for $j = 1, 2, 3, \ldots, N_c$ and $u = 1, 2, 3, \ldots, N_u$. Hence, s_{ju} will be set to "1" if the u^{th} GU asks for the j^{th} content, otherwise, it will be set to "0". To further illustrate the format of $\boldsymbol{S}$, an example that considers 6 GUs with totally 4 contents is included. Firstly, the contents requested by 6 GUs is $\{c_1, c_4, c_3, c_4, c_2, c_4\}$ and the order of these contents is arranged sequentially based on the index of GUs. As a result, the selection matrix for this example is given by:

$$\boldsymbol{S} = \begin{bmatrix} 1 & 0 & 0 & 0 & 0 & 0 \\ 0 & 0 & 0 & 0 & 1 & 0 \\ 0 & 0 & 1 & 0 & 0 & 0 \\ 0 & 1 & 0 & 1 & 0 & 1 \end{bmatrix}. \tag{10}$$

It can be seen that the first, the second and the third contents are requested once by the first, the fifth and the third GUs, respectively. While the forth content is three times requested by the other GUs. Therefore, the position of the requested content in each column of the corresponding GU is set to "1", while the rest will be set to "0".

Since all the factors that will be used have been provided, the derivation of data rate in our proposed CS-OFDMA communication system will be detailed in the following by two scenarios:

1) Scenario 1: In the first scenario of CS-OFDMA, we consider that the private message has a higher power allocation in each subcarrier. Besides, since the bandwidth assigned to

each GU is equally divided, the bandwidth is removed from the equations in the following sections. Consequently, the private rate R_p^i and the common rate R_c^i of the i^{th} subcarrier can be given by:

$$R_p^i = \log_2\left(1 + \frac{|h_i|^2(1-p_i)}{|h_i|^2 p_i + \sigma^2}\right), \tag{11}$$

$$R_c^i = A_i \log_2\left(1 + \frac{|h_T|^2 p_i}{\sigma^2}\right). \tag{12}$$

Again, h_i is the metric that is used to modulated the private message at the i^{th} subcarrier. While $A_i = \boldsymbol{W}_i \boldsymbol{S} \boldsymbol{F}_i$ is a coefficient for the utilization measurement of common message in the i^{th} subcarrier named by "sharing times". Back to the definition of A_i, it can be found that $\boldsymbol{W}_i$ represents the proportion of each content, $\boldsymbol{S}$ links the GUs to their corresponding content and $\boldsymbol{F}_i$ helps to find out the accessible GUs of the i^{th} subcarrier. Therefore, the sharing times of each content can be obtained based on the proportion of each content and the number of accessible GUs requesting for this content. Accordingly, it is straightforward to see that A_i is actually the sum sharing times of all contents carried by the i^{th} subcarrier. Therefore, the sum rate of the i^{th} subcarrier can be obtained by:

$$\begin{aligned} R_s^i &= R_p^i + R_c^i \\ &= A_i \log_2\left(|h_T|^2 p_i + \sigma^2\right) - \log_2\left(|h_i|^2 p_i + \sigma^2\right) + \mathcal{C}_1, \end{aligned} \tag{13}$$

where $\mathcal{C}_1 = \log_2\left(|h_i|^2 + \sigma^2\right) - A_i \log_2\left(\sigma^2\right)$. Then, the derivative of R_s^i with respect to p_i can be calculated as:

$$\frac{\partial R_s^i}{\partial p_i} = \frac{A_i |h_T|^2}{|h_T|^2 p_i + \sigma^2} - \frac{|h_i|^2}{|h_i|^2 p_i + \sigma^2}. \tag{14}$$

Hence, the extremum p_e of the power allocation coefficient p_i for R_s^i can be obtained by setting $\frac{\partial R_s^i}{\partial p_i} = 0$, which is given by:

$$p_e = \frac{|h_i|^2 - A_i |h_T|^2}{A_i - 1} \cdot \frac{\sigma^2}{|h_T|^2 |h_i|^2}. \tag{15}$$

Since $A_i \geq 1$, we have three conditions if $|h_T|^2 < \frac{\sigma^2}{A_i - 1}$:

$$\begin{cases} p_e > 1, & \text{if } |h_i|^2 > \frac{A_i |h_T|^2 \sigma^2}{\sigma^2 - (A_i - 1)|h_T|^2}; \\ 0 \leq p_e \leq 1, & \text{if } A_i |h_T|^2 \leq |h_i|^2 \leq \frac{A_i |h_T|^2 \sigma^2}{\sigma^2 - (A_i - 1)|h_T|^2}; \\ p_e < 0, & \text{if } |h_i|^2 < A_i |h_T|^2. \end{cases} \tag{16}$$

However, it always satisfies the condition that $p_e \leq 1$ if $|h_T|^2 \geq \frac{\sigma^2}{A_i - 1}$. Hence, we have:

$$\begin{cases} 0 \leq p_e \leq 1, & \text{if } |h_i|^2 \geq A_i |h_T|^2; \\ p_e < 0, & \text{if } |h_i|^2 < A_i |h_T|^2. \end{cases} \tag{17}$$

According to the above derivation, if we aim to maximize the sum rate of all users, $p_i = 1$ as R_s^i is monotonically increasing when $p_e < 0$, while $p_i = 0$ as R_s^i is monotonically decreasing when $p_e > 1$. Moreover, the montonicity of R_s^i when $0 \leq p_e \leq 1$ indicates that the maximum value of R_s^i can be achieved at either "0" or "1" since it is monotonically decreasing from "0" to "p_e" and only one extremum p_e is obtained. In summary, the value of p_i must satisfy the following constraint:

$$\begin{cases} p_i = 0, & \text{if } p_e > 1; \\ p_i = 1, & \text{if } p_e < 0; \\ p_i = \underset{p_i \in \{0,1\}}{\arg\max}\, R_s^i(p_i), & \text{if } 0 \leq p_e \leq 1. \end{cases} \tag{18}$$

2) Scenario 2: The second scenario considers the case that the common part has a higher power allocation with power allocation coefficient $1 - p_i'$. Therefore, the private rate $R_p^{i'}$ and the common rate $R_c^{i'}$ of the i^{th} subcarrier are given by:

$$R_p^{i'} = \log_2\left(1 + \frac{|h_i|^2 p_i'}{\sigma^2}\right), \tag{19}$$

$$R_c^{i'} = A_i \log_2\left(1 + \frac{|h_T|^2(1-p_i')}{|h_T|^2 p_i' + \sigma^2}\right). \tag{20}$$

Accordingly, the sum rate of the i^{th} subcarrier can be expressed by:

$$\begin{aligned} R_s^{i'} &= R_p^{i'} + R_c^{i'} \\ &= -A_i \log_2\left(|h_T|^2 p_i' + \sigma^2\right) + \log_2\left(|h_i|^2 p_i' + \sigma^2\right) + \mathcal{C}_2, \end{aligned} \tag{21}$$

where $\mathcal{C}_2 = A_i \log_2\left(|h_T|^2 + \sigma^2\right) - \log_2\left(\sigma^2\right)$. Similarly, based on the monotonicity of R_s^i in different conditions, if we aim to maximize the sum rate of all users, the value of p_i' must satisfy the following constraint:

$$\begin{cases} p_i' = 1, & \text{if } p_e' > 1; \\ p_i' = 0, & \text{if } p_e' < 0; \\ p_i' = \underset{p_i' \in \{0,1\}}{\arg\max}\, R_s^{i'}(p_i'), & \text{if } 0 \leq p_e' \leq 1. \end{cases} \tag{22}$$

Therefore, it could be found that the power allocation coefficient is either 1 or 0 based on (18) and (22), which means that the i^{th} subcarrier should transmit all private message or all common message based on the condition of the threshold h_T and the channel gain of the i^{th} subcarrier h_i. In other words, the subcarrier should serve GUs either privately or publicly based on the channel condition, and hence there is no combination of them to serve GUs in a hybrid way. Inspired by this results, the idea of directly sharing the contents in subcarriers among all GUs to increase the utilization of limited bandwidth resources is proposed. In the following two sections, two CS schemes will be introduced in details.

C. Proposed Private Content-Sharing Scheme

The first CS scheme is inspired from the first conclusion of CS-OFDMA, namely each subcarrier will only carry the information of the content that is requested by its corresponding GU. Therefore, it can be found that this scheme is operated in a relatively "private" way, which can be referred to as private CS (PCS).

As shown Fig. 4 the subcarriers that carried the same kind of contents have been marked by the same colors in CS scheme. Instead of considering to transmit the contents in a hybrid way (private and common), the system directly shares the contents requested by each GU. As a result, the data rate

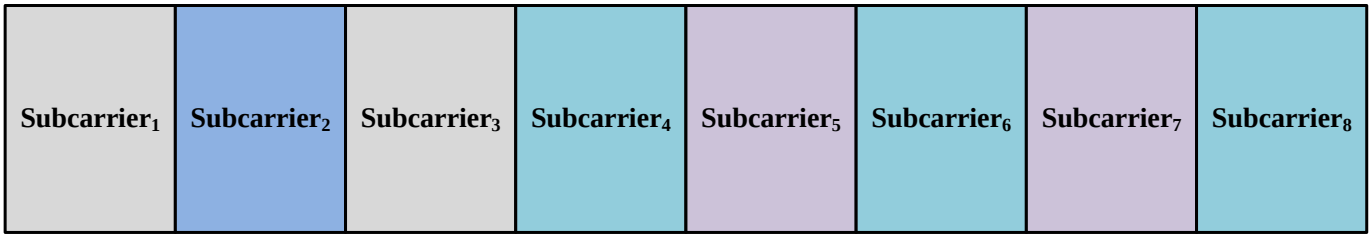

Fig. 4: Illustration of PCS in the frequency domain of OFDMA communication system.

could be improved if we allow those GUs who request the same content to share their contents with each other. For instance, we take the GUs who are requesting the same "Grey" content in the first and third subcarriers as an example, if the corresponding two GUs can only demodulate their allocated subcarriers, the same data need to be transmitted repeatedly on their subcarriers. However, the data rate can be increased if they are allowed to share their subcarriers, because the UAV can now transmit two packages of this content. Here, it is worth noting that the content need to be transmitted by several data packages. Therefore, the GU with a higher channel gain can directly obtain the first data from the GU that has a lower channel gain and obtain the second one by his own subcarrier, which means the GUs with higher channel gain can utilize the data package from other GUs who requested the same content and reduce the duplicate transmissions.

So far, it is straightforward to see that most of the subcarriers can be shared by other GUs if available. In order to calculate the average data rate of the PCS scheme, we take the $4^{th}, 6^{th}$ and 8^{th} subcarriers that all requested the "Aqua" content in Fig. 4 and we assume that the achievable rate of each subcarrier is in the descending order of 4-6-8. Then, the corresponding sharing times of these 3 subcarriers is 1, 2 and 3, because only these 3 GUs need this content while the others do not. It could be found that the utilization of subcarriers is significantly improved. Finally, the average rate R_A of all GUs in PCS transmission scheme can be formulated as:

$$R_A = \frac{1}{N_u} \sum_{i=1}^{N_s} A_i \log_2 \left(1 + \frac{|h_i|^2}{\sigma^2}\right), \tag{23}$$

where A_i is the sum sharing times of the i^{th} subcarrier. However, to further improve the average data rate of PCS, we propose an advanced CS method, referred to as common CS (CCS).

D. Proposed Common Content-Sharing Scheme

As mentioned before, the GU in PCS can only obtain the information from the subcarriers of GUs that request the same content but have weaker received signal strength. However, GUs will not be restricted by the category of contents since all subcarriers are able to carry all related contents in a pure "common" way, which means GUs are capable of demodulating all available subcarriers. Then, the utilization of each subcarrier can be further improved. Besides, the data rate can also be controlled by adjusting the proportion of contents in each subcarrier. Here, an example of one subcarrier with 5 contents represented by different colors is shown in Fig. 5 to illustrate the format of CCS in one subcarrier, where the message is composed by all contents considered in the system but different proportion.

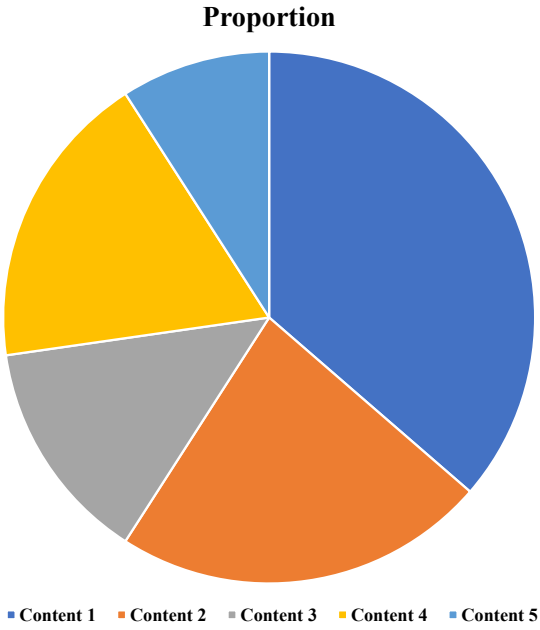

Fig. 5: An example of content proportion in one subcarrier with 5 contents.

Similar to the common part in CS-OFDMA, a filter vector $\boldsymbol{F}_i$ is used to select those accessible GUs for the i^{th} subcarrier. Accordingly, the rate of the i^{th} subcarrier in CCS scheme can be calculated by:

$$R_i = \boldsymbol{W}_i \boldsymbol{S} \boldsymbol{F}_i \log_2 \left(1 + \frac{|h_i|^2}{\sigma^2}\right) = A_i \log_2 \left(1 + \frac{|h_i|^2}{\sigma^2}\right), \tag{24}$$

where $A_i = \boldsymbol{W}_i \boldsymbol{S} \boldsymbol{F}_i$ is the sharing times of the i^{th} subcarrier in CCS scheme. Here, Note here that the difference between PCS and CCS is the calculation of the sharing times. Consequently, the average data rate R_A of the CCS scheme can also be expressed by (23).

Our objective is to maximize the average data rate R_A by optimizing the weight vector of each subcarrier, under the weight constraint $\sum_{j=1}^{N_c} w_{ij} = 1$ and the individual minimum rate requirement $\mathrm{R}_{\min}$ of the GUs. Hence, it is necessary to formulate the rate of each GU before the optimization, where the rate of the u^{th} GU is defined by R_u. Since R_u is related to different components of one content in each subcarrier,

a content based weight vector $\tilde{\boldsymbol{W}}_j$ is then given by $\tilde{\boldsymbol{W}}_j = [w_{1j}, w_{2j}, \ldots, w_{ij}, \ldots, w_{N_s j}]^T$, for $j = 1, 2, 3, \ldots, N_c$, where w_{ij} is the weight of the j^{th} content in the i^{th} subcarrier. Similar to $\boldsymbol{W}_i$, the weight vector of the u^{th} GU across all subcarriers is given by $\boldsymbol{W}_u \in \mathcal{W}_J = \left\{\tilde{\boldsymbol{W}}_1, \tilde{\boldsymbol{W}}_2, \ldots, \tilde{\boldsymbol{W}}_j, \ldots, \tilde{\boldsymbol{W}}_{N_c}\right\}$. Here, it is worth noting that $\boldsymbol{W}_u$ is selected based on the content requested by the u^{th} GU.

Besides, the vector $\boldsymbol{V}$ that indicates the achievable rate of each subcarrier has the following form $\boldsymbol{V} = [v_1, v_2, \ldots, v_i, \ldots, v_{N_s}]^T$, where v_i is the achievable rate of the i^{th} subcarrier obtained by (5). Then, the rate of the u^{th} GU can be written accordingly as:

$$R_u = \boldsymbol{W}_u^T \left(\boldsymbol{F}_u \odot \boldsymbol{V}\right), \tag{25}$$

where $\boldsymbol{F}_u \in \mathbb{C}^{N_s \times 1}$ is the filter vector of the u^{th} GU and the symbol $\odot$ denotes the Hadamard product. Here, $\boldsymbol{F}_u$ is used to filter out the subcarriers that the u^{th} GU can access. For example, if we consider a group of 6 GUs and $|h_1|^2 > |h_2|^2 > |h_3|^2 > |h_4|^2 > |h_5|^2 > |h_6|^2$, then, the third GU's filter vector can be represented by $\boldsymbol{F}_3 = [0, 0, 1, 1, 1, 1]^T$. Hence, a weight matrix $\boldsymbol{W} \in \mathbb{C}^{N_s \times N_c}$ that includes all weight elements is given by:

$$\boldsymbol{W} = \begin{bmatrix} \boldsymbol{W}_1 \\ \boldsymbol{W}_2 \\ \vdots \\ \boldsymbol{W}_i \\ \vdots \\ \boldsymbol{W}_{N_s} \end{bmatrix} = \begin{bmatrix} \tilde{\boldsymbol{W}}_1 & \tilde{\boldsymbol{W}}_2 & \cdots & \tilde{\boldsymbol{W}}_j & \cdots & \tilde{\boldsymbol{W}}_{N_c} \end{bmatrix}, \tag{26}$$

for $\boldsymbol{W}_i \in \mathcal{W}_I$ and $\tilde{\boldsymbol{W}}_j \in \mathcal{W}_J$. As a result, it can be seen that $\boldsymbol{W}_i$ is the row vector of $\boldsymbol{W}$ and $\tilde{\boldsymbol{W}}_j$ is the column vector of $\boldsymbol{W}$. Also, $\boldsymbol{N}_i^T = \boldsymbol{S}\boldsymbol{F}_i$ is a vector that represents the number of accessible GUs requesting each content in the i^{th} subcarrier, which is given by $\boldsymbol{N}_i = [n_{i1}, n_{i2}, \ldots, n_{ij}, \ldots, n_{iN_c}]$, where n_{ij} is the number of accessible GUs requesting the j^{th} content in the i^{th} subcarrier. Moreover, we define a vector $\boldsymbol{f} = [v_1\boldsymbol{N}_1, v_2\boldsymbol{N}_2, \ldots, v_i\boldsymbol{N}_i]^T$, for $v_i \in \boldsymbol{V}$. Finally, the average data rate of CCS can be represented by:

$$R_A = \frac{1}{N_u} \sum_{i=1}^{N_s} A_i \log_2 \left(1 + \frac{|h_i|^2}{\sigma^2}\right) = \frac{1}{N_u} \boldsymbol{f}^T \boldsymbol{vec}\left(\boldsymbol{W}\right), \tag{27}$$

where $\boldsymbol{vec}\left(\cdot\right)$ is an operator to vectorize a target matrix into a column vector based on the row of the target matrix. As a result, it can be found that the optimization of the average data rate in the CCS is translated into a linear programming problem by adjusting the weight of contents in each subcarrier [59]. Mathematically, the average data rate maximization problem can be formulated as:

$$\max_{\boldsymbol{W}} R_A \iff \max_{\boldsymbol{W}} \boldsymbol{f}^T \boldsymbol{vec}\left(\boldsymbol{W}\right), \ \boldsymbol{s.t.} \begin{cases} 0 \le w_{ij} \le 1, \\ \sum_{j=1}^{N_c} w_{ij} = 1, \\ R_u \ge R_{\min}. \end{cases} \tag{28}$$

III. UAV Deployment

In the case of a UAV-assisted communication system, the advantages of rapid establishment and controlled mobility should be utilized to enhance the communication quality of GUs when compared with traditional fixed terrestrial BSs. Therefore, we propose two different deployment schemes to optimize the average rate of our proposed CS transmission schemes by utilizing the content awareness. Here, we need to emphasize that the user association [60], [61] has been completed before UAV deployment, which is considered according to the associated GUs. Then, the data transmission will be conducted after the UAV deployment. Hence, a one-UAV scenario is provided here to illustrate the process of UAV deployment. Firstly, inspired from the traditional k-means clustering algorithm, a fixed-point based deployment scheme is designed for the PCS transmission scheme. Afterwards, a traverse-search based deployment is proposed for the CCS transmission scheme.

Here, we consider a LoS dominant communication environment in our UAV-assisted communication system, which means that the received signal power is determined by the path loss between the UAV and the GUs. Besides, the time scales of UAV deployment is much larger than that of fast fading, which means the h_{NLoS} is rapidly changing during the process of deployment. Since we cannot keep up with the changes of h_{NLoS}, only the h_{LoS} and the path loss are considered to optimize the deployment of UAV. Firstly, we assume that the UAV is flying at a fixed height of h_d, and the coordinate of the UAV can be expressed by $\boldsymbol{G} = [x_a, y_a, h_d]$. Similarly, the coordinate of the u^{th} GU can be represented by $\boldsymbol{U}_u = [x_u, y_u, 0]$. Here, the height of GUs is negligible compared with the A2G distance. Additionally, we also define the terrestrial coordinates $\tilde{\boldsymbol{G}} = [x_a, y_a]$ and $\tilde{\boldsymbol{U}}_u = [x_u, y_u]$ to represent the terrestrial coordinates of the UAV and the GUs, respectively. Therefore, the A2G distance d_u between the u^{th} GU and the UAV is given by:

$$d_u = \|\boldsymbol{G} - \boldsymbol{U}_u\| = \sqrt{\left(x_a - x_u\right)^2 + \left(y_a - y_u\right)^2 + h_d^2}. \tag{29}$$

Additionally, h_{LoS} can be expressed by $h_{\text{LoS}} = e^{-j\frac{2\pi}{\lambda}d}$ [62], where d is the distance in meter between the transmitter and the receiver. Consequently, the received signal power of the u^{th} GU in the LoS dominant environment is given by:

$$P_{r_s} = P_t |h_{\text{LoS}}|^2 \left(\frac{c}{4\pi d_u f_c}\right)^2 = P_t \left(\frac{c}{4\pi d_u f_c}\right)^2. \tag{30}$$

The traditional k-means clustering algorithm uses the squared Euclidean distance to find out the mean of the points in that cluster iteratively. Here, we choose the achievable rate as the "distance metric" in our PCS based communication system, where the deployment of the UAV can be transformed to the following optimisation problem:

$$\max_{\tilde{\boldsymbol{G}}} \sum_{u=1}^{N_u} A_u \log_2 \left(1 + \frac{P_t}{\sigma^2} \left(\frac{4\pi f_c \|\boldsymbol{G} - \boldsymbol{U}_u\|}{c}\right)^{-\alpha}\right), \tag{31}$$

where A_u is the sharing times of the u^{th} subcarrier, while $\tilde{\boldsymbol{G}}$ is the ground coordinates of the UAV and can be represented

by $\tilde{\boldsymbol{G}} = (x_a, y_a)$. Furthermore, the transmit power P_t is large enough to cover all GUs in the target area, which means the received signal to noise power ratio (SNR) is high. Therefore, we may use the following approximation:

$$\max_{\tilde{\boldsymbol{G}}} \sum_{u=1}^{N_u} A_u \log_2 \left(\frac{P_t}{\sigma^2} \left(\frac{4\pi f_c \|\boldsymbol{G} - \boldsymbol{U}_u\|}{c} \right)^{-\alpha} \right), \quad (32)$$

which is equivalent to:

$$\max_{\tilde{\boldsymbol{G}}} -\alpha \sum_{u=1}^{N_u} A_u \log_2 \|\boldsymbol{G} - \boldsymbol{U}_u\|. \quad (33)$$

As mentioned before, the free space path loss exponent $\alpha = 2$ is selected in the LoS dominant environment. Thus, (33) can be further simplified as:

$$\min_{\tilde{\boldsymbol{G}}} \sum_{u=1}^{N_u} A_u \log_2 \|\boldsymbol{G} - \boldsymbol{U}_u\|^2. \quad (34)$$

Taking the gradient with respect to $\boldsymbol{G}$ and setting it to zero, we get $\sum_{u=1}^{N_u} \frac{A_u(\tilde{\boldsymbol{G}} - \tilde{\boldsymbol{U}}_u)}{\|\boldsymbol{G} - \boldsymbol{U}_u\|^2} = \boldsymbol{0}$. Then, simplifying this equation, we obtain:

$$\tilde{\boldsymbol{G}} = \frac{\sum_{u=1}^{N_u} \frac{A_u \tilde{\boldsymbol{U}}_u}{\|\boldsymbol{G} - \boldsymbol{U}_u\|^2}}{\sum_{u=1}^{N_u} \frac{A_u}{\|\boldsymbol{G} - \boldsymbol{U}_u\|^2}}. \quad (35)$$

Afterwards, we use fixed-point iteration to obtain the solution as follow [46]:

$$\tilde{\boldsymbol{G}}^{(t+1)} = \frac{\sum_{u=1}^{N_u} \frac{A_u \tilde{\boldsymbol{U}}_u}{\|\boldsymbol{G}^{(t)} - \boldsymbol{U}_u\|^2}}{\sum_{u=1}^{N_u} \frac{A_u}{\|\boldsymbol{G}^{(t)} - \boldsymbol{U}_u\|^2}}. \quad (36)$$

It can be seen that $\tilde{\boldsymbol{G}}$ is the linear combination of $\tilde{\boldsymbol{U}}_u$, where $\tilde{\boldsymbol{U}}_u$ is a convex hull. Therefore, the UAV will be restricted in the convex hull (target area) and will be rapidly dragged into the convex hull even if the initial point is selected outside the convex hull. Furthermore, we set $\boldsymbol{E} = \frac{A_u(\tilde{\boldsymbol{G}} - \tilde{\boldsymbol{U}}_u)}{\|\boldsymbol{G} - \boldsymbol{U}_u\|^2}$ and the Hessian matrix with respect to $\boldsymbol{G}$ based on $\boldsymbol{E}$ can be expressed by:

$$\begin{aligned} \frac{\partial \boldsymbol{E}}{\partial \boldsymbol{G}} &= \frac{A_u \left(2\boldsymbol{I} \|\boldsymbol{G} - \boldsymbol{U}_u\|^2 - 4(\tilde{\boldsymbol{G}} - \tilde{\boldsymbol{U}}_u)(\tilde{\boldsymbol{G}} - \tilde{\boldsymbol{U}}_u)^T \right)}{\|\boldsymbol{G} - \boldsymbol{U}_u\|^4}, \\ &= \frac{A_u \left(2\boldsymbol{I} \|\boldsymbol{G} - \boldsymbol{U}_u\|^2 - 4\|\tilde{\boldsymbol{G}} - \tilde{\boldsymbol{U}}_u\|^2 \boldsymbol{Z}\boldsymbol{Z}^T \right)}{\|\boldsymbol{G} - \boldsymbol{U}_u\|^4}, \end{aligned} \quad (37)$$

where $\boldsymbol{Z} = \frac{\tilde{\boldsymbol{G}} - \tilde{\boldsymbol{U}}_u}{\|\tilde{\boldsymbol{G}} - \tilde{\boldsymbol{U}}_u\|}$ is the direction vector of $\tilde{\boldsymbol{G}} - \tilde{\boldsymbol{U}}_u$, which can also be represented in parametric form as: $\boldsymbol{Z} = [\cos\theta, \sin\theta]$ and the direction angle θ can be obtained by $\theta = \arccos(\cos\theta)$. However, the Hessian matrix will be positive definite only when enough number of GUs are in the target area, otherwise, it cannot be determined. Additionally, it is worth noting that the expectation of $\boldsymbol{Z}\boldsymbol{Z}^T$ with respect to the direction angle θ satisfies the following condition:

$$\mathbb{E}_\theta \left\{ \boldsymbol{Z}\boldsymbol{Z}^T \right\} = \begin{bmatrix} \cos\theta^2 & \cos\theta\sin\theta \\ \cos\theta\sin\theta & \sin\theta^2 \end{bmatrix} = \frac{1}{2}\boldsymbol{I}, \quad (38)$$

when a large number of GUs are distributed in the target area. According to (37) and (38), we take the expectation of (37) with respect to the direction angle θ as:

$$\begin{aligned} \mathbb{E}_\theta \left\{ \frac{\partial \boldsymbol{E}}{\partial \boldsymbol{G}} \right\} &= \frac{2A_u \boldsymbol{I}}{\|\boldsymbol{G} - \boldsymbol{U}_u\|^4} \left(\|\boldsymbol{G} - \boldsymbol{U}_u\|^2 - \|\tilde{\boldsymbol{G}} - \tilde{\boldsymbol{U}}_u\|^2 \right) \\ &= \frac{2A_u \boldsymbol{I} h_d^2}{\|\boldsymbol{G} - \boldsymbol{U}_u\|^4}. \end{aligned} \quad (39)$$

Therefore, it can be proved that (39) is positive definite and the objective function (34) is convex when a large number of GUs are distributed in the target area, which means that the proposed deployment can always "converge" to the global optimum position.

The above deployment process is also applicable in the classic OFDMA scenarios, where non-content-sharing (NCS) is employed, by simply setting the coefficient A_u to 1. Here, it can be found that the sum of A_u in both of the cases is a constant no matter how the location of the UAV changes. To further illustrate this phenomenon, we consider that three GUs request the same content under this condition. Then, the corresponding sharing times A_u must be one of the cases illustrated by Table I based on the order of received signal power. Therefore, it is clear that the sum of A_u is always a constant even during the process of deployment, i.e. $\sum_u^{N_u} A_u = 6$.

TABLE I: The combinations of weight vector when 3 GUs request the same content in content-sharing scheme.

w_1	1	1	2	2	3	3
w_2	2	3	1	3	1	2
w_3	3	2	3	1	2	1

However, this is not the case in the CCS scenario. It is known to us that the contents in each subcarrier as well as the weight of each content will be obtained simultaneously by linear programming. This means the A_u in CCS case keeps changing when the UAV is moving. In other words, the gradients of different locations are different, which results in disabling the fixed-point iteration. At different locations, the optimization process cannot guarantee that the weight vector $\boldsymbol{W}_i$ is fixed because different positions will result in different rates for the GU. Therefore, to meet the demand of the basic data requirement $\mathrm{R}_{\min}$, the system has to adjust the weight of each content, which will result in varying the weight vector. Besides, the change of locations will also change the filter vector and further affect the sharing times A_u. Moreover, it can be found from (36) that the update of the UAV's location is based on the sharing times and the previous location of the UAV, which means the update of the UAV's location based on (36) does not work when the sharing times keeps changing in the CCS.

As shown in Fig. 6(a), the sum of sharing times at different deployment locations of the UAV in a scenario of 50 GUs in a 1 km $\times$ 1 km target area is varying at different places. Also, the red point in Fig. 6(a) indicates the position that produces the highest sum of A_u. Since the sharing times is related to the location of the UAV, the deployment scheme proposed in PCS scheme is not applicable for the CCS

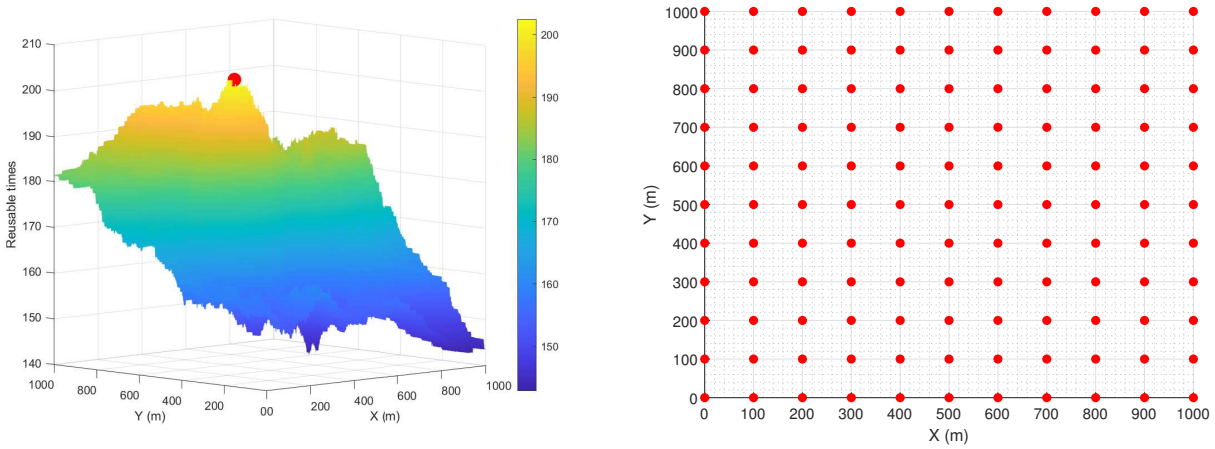

(a) Sum of sharing times.

(b) Grids on the ground.

Fig. 6: The sum of sharing times in CCS scenario at different deployment locations in 1 km $\times$ 1 km area with 50 GUs.

case any more. Therefore, we design a traverse-search based deployment scheme for our proposed CCS scenario. Firstly, we divide the whole target area into small grids as shown in Fig. 6(b). Afterwards, all possible locations (points) are tested and then the point achieving the maximum average data rate, as illustrated in Fig. 6(a), is selected as the final deployment location. Consequently, the computation complexity is directly related to the size of the grids. Fortunately, this procedure can be accomplished by sending the location information back to the terrestrial BS via backhaul links as the computation ability of terrestrial BS is much stronger than that on the UAV or it can also be accomplished by the UAV itself if the UAV's computation capability is good enough to support this process.

IV. Simulation Results

In this section, we investigate the performance of our proposed content-aware communication system in a 1 km $\times$ 1 km square area with a total of $N_u = 50$ GUs uniformly distributed on the ground. Besides, the UAV flies at a height of $h_d = 100$ m and operate at a frequency band of $f_c = 5.8$ GHz for the A2G communication. Under the LoS model, the path loss exponent α is set to 2. Meanwhile, the noise PSD N_0 is set to -174 dBm/Hz and the transmission power P_t of the UAVs is 26 dBm. Additionally, OFDMA is employed to support multi-user communications, where the total bandwidth B allocated to all GUs is 40 MHz. In our system, the whole bandwidth is equally divided into $N_s = 50$ subcarriers and each GU will be assigned one subcarrier. Moreover, we assume that the interests of GUs are stable within a long period, which means the distribution of GUs interests is fixed in our simulation time[3]. In the following, we first analyze the effect of the UAV deployment based on the average rate of all GUs. Afterwards, the average rate of each transmission scheme will be investigated. The detailed simulation parameters are listed in Table II.

In our proposed CS transmission schemes, the average rate of each GU is taken as the objective function for optimising the UAV deployment. Fig. 7 depicts the performance of our proposed deployment schemes in the scenario of one UAV with 50 associated GUs in its target area. In our simulation, we tested 3 different deployment schemes, which are classic k-means algorithm, fixed-point algorithm and traverse-search algorithm. In Fig. 7, the fixed-point deployment scheme is applied on two scenarios, where we use NCS to indicate the scenario that uses fixed-point deployment without CS transmission scheme, while use PCS to indicate the scenario that uses fixed-point deployment with PCS transmission scheme. Then, CCS is used to illustrate the deployment by traverse-search algorithm with CCS transmission scheme. Moreover, in order to reveal the generality of our proposed deployment scheme, we randomly set the initial points of the fixed-point deployment scheme with two different setups as seen in Fig. 7(a) and Fig. 7(b). Here, two different setups means the locations of GUs and the requested contents are different. Additionally, the GUs are classified by the requested times of contents, which is pointed out by the number in the legend. For example, those GUs marked by small blue "$\triangledown$" in Fig. 7(a) means that their requested contents occurred only once, but it is worth noting that the same requested times does not mean they requested the same content.

As shown in Fig. 7(a) and Fig. 7(b), we consider a scenario with 50 GUs in a target area served by one UAV with different deployment schemes under the constraint of $\mathrm{R}_{\min} = 0.5$ and 9.5 Mbits/s, where CCS_1 is the final deployment location when $\mathrm{R}_{\min} = 0.5$ Mbits/s and CCS_2 is the final deployment location when $\mathrm{R}_{\min} = 9.5$ Mbits/s. It can be seen that the final deployment locations of k-means and fixed-point without CS are very close in a LoS dominant environment, which means the distance based and average rate based deployment schemes offer similar results as the rate is directly related to the A2G distances in a LoS environment. Besides, the sharing times

[3] The UAV has to request the new contents from the core network if new contents are requested by GUs. Therefore, this will cause a request delay since the new contents have not been cached in advance but the proposed transmission scheme can still be applied when the new contents are obtained.

TABLE II: Simulation parameters

Parameter	Symbol	Value	Parameter	Symbol	Value
Bandwidth	B	40 MHz	Noise PSD	N_0	-174 dBm/Hz
Carrier frequency	f_c	5.8 GHz	Path loss exponent	α	2
Transmission power	P_t	26 dBm	UAV height	h_d	100 m
Speed of light	c	3×10^8 m/s	Number of contents	N_c	50
Number of GUs	N_u	50	Number of subcarriers	N_s	50

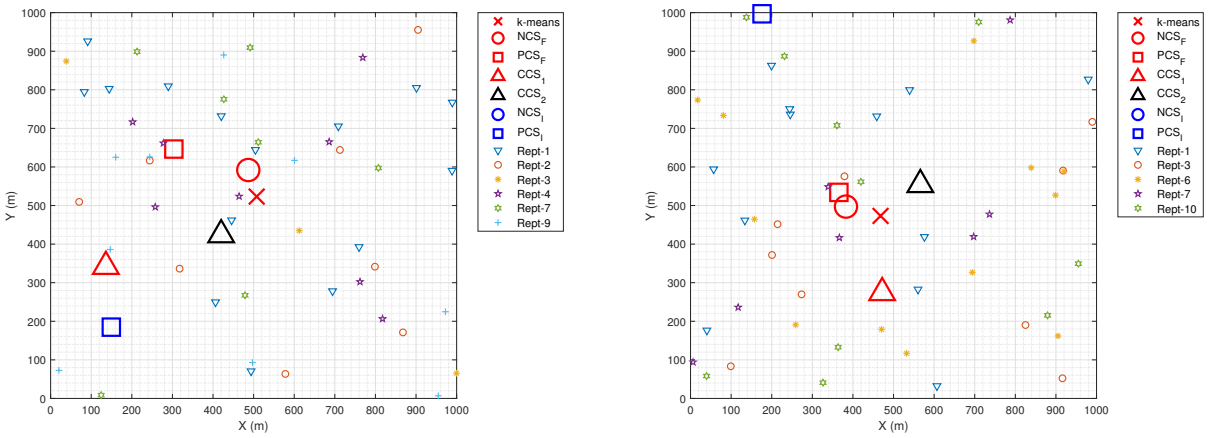

(a) Setup 1.

(b) Setup 2.

Fig. 7: Illustration of the UAV deployment with 50 GUs and $\mathrm{R}_{\min} = 0.5$ and 9.5 Mbits/s by the proposed deployment algorithm, where NCS, PCS and CCS denote non-content-sharing, private content-sharing and common content-sharing, respectively. While the repetition-x indicates the requested times of contents for GUs represented by the same markers is x. Moreover, the subscripts I and F indicate the initial locations and the final locations, respectively.

of the contents, which are indicated by repetition-x in Fig. 7, plays an important role in the deployment of UAV in each setup. Compared to the first two deployment schemes that stay at around the centroids of all GUs, the final deployment position of PCS is more biased to those GUs with contents that have high sharing times. In both setups, if we focus on the GUs of "Rept-9" in Setup 1 and the GUs of "Rept-10" in Setup 2, the final positions of PCS are around the center of this two groups. However, the deployment CCS is accomplished based on an exhaustive search of the whole area based on the threshold $\mathrm{R}_{\min}$. Then, unlike PCS, CCS does not show any bias to specific group of GUs as the final position is also controlled by the repeated times and the rate of GUs. Again, there is a need to emphasize that the rates at different locations are different. Thus, this results in the weight obtained from the optimization to vary at different locations, which further causes the variation of sharing times. As a result, it is hard to conclude that the deployment of UAV in CCS will bias to any specific group. Nevertheless, if we focus on the final deployment positions of the two minimum values in both setups, the deployment position of small threshold is usually far from the centroids of those GUs, while the deployment position of high threshold is usually around the centroid of those GUs. This is because the small threshold will sacrifice the performance of those GUs with low-frequency requested contents to increase the overall performance. As a result, the deployment position should be far from those GUs with low-frequency requested contents but close to those GUs with high-frequency requested contents. On the contrary, a high threshold means those GUs with high-frequency requested contents have to "allocate" part of their rate to those GUs with low-frequency requested contents, which means the optimization will finally find a balanced place and this place is usually around the centroid of all GUs.

Additionally, Fig. 8 illustrates the convergence progress of fixed-point deployment algorithm in NCS scenario. For conciseness, the scenario of PCS will not be repeatedly illustrated here to show the same property. It can be found from Fig. 8(a) and Fig. 8(b) that two different initial points (within and outside convex hull) have been selected to test the performance of the proposed fixed-point deployment scheme in the same distribution of GUs. These two figures show that the UAVs will iteratively converge to the final deployment position no matter where the initial point is selected. Besides, it can be seen that the convergence is very fast. If we consider other iterative algorithm, such as gradient algorithm, the speed of convergence will be very slow when the step size is too small. On the other hand, the final results may not be satisfactory if the step size is too big. Therefore, our proposed deployment scheme can rapidly and precisely find the position where the maximum average rate can be achieved.

In Fig. 9, the average SE is obtained by Monte Carlo simulation, where we run a large number of setups with different locations of GUs with different requested contents for testing the performance of our system. Fig. 9(a) shows the average SE of different investigated transmission schemes. Here, the data transmission will always be conducted after the deployment of UAV, which implys that the deployment has been considereded

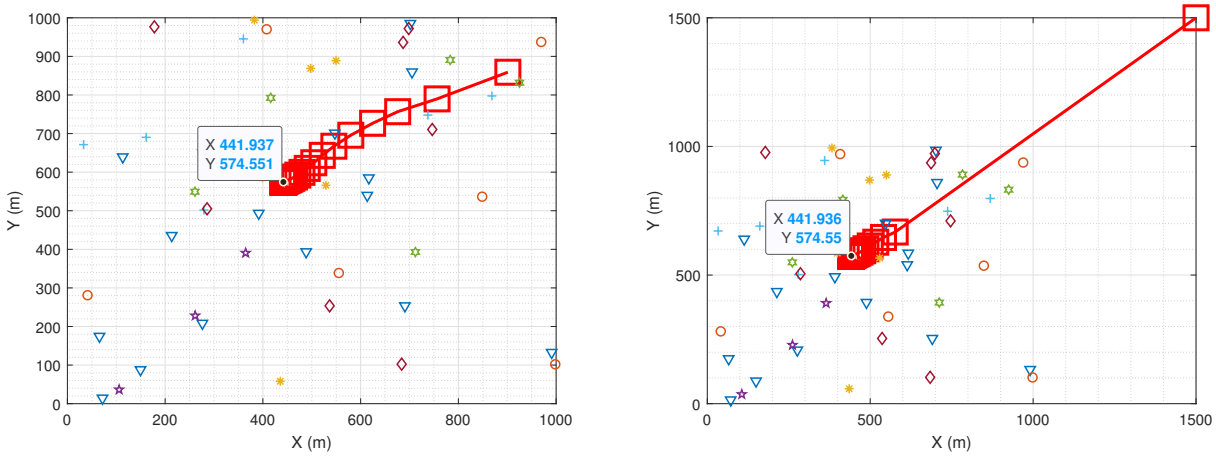

(a) Within convex hull.

(b) Outside convex hull.

Fig. 8: Convergence progress of the UAV deployment with 50 GUs by fixed-point deployment algorithm in NCS method.

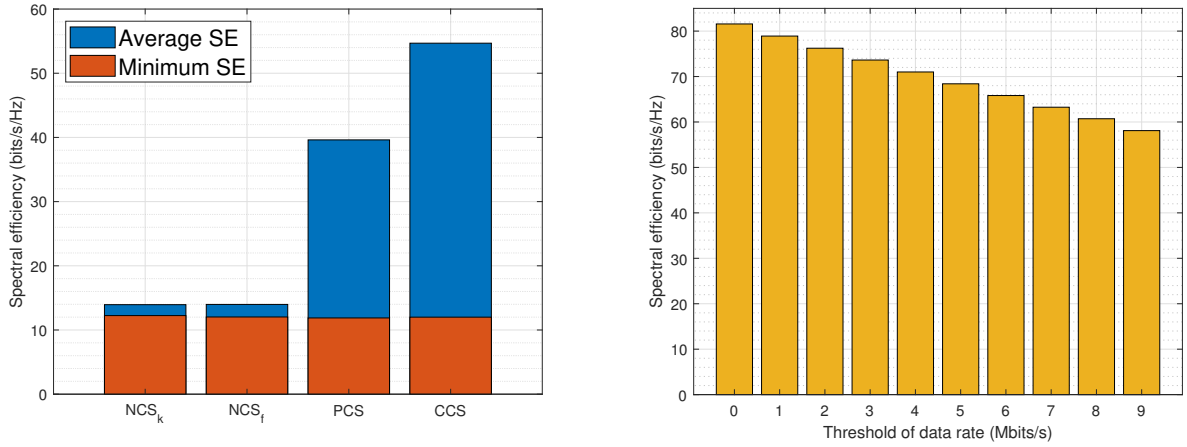

(a) Comparison of average spectral efficiency.

(b) Average spectral efficiency of different thresholds.

Fig. 9: Illustration of the average spectral efficiency by different deployment schemes and transmission schemes, where $\mathrm{NCS_k}$ and $\mathrm{NCS_f}$ indicate the NCS transmission schemes that are deployed by k-means and fixed-point, respectively.

when discuss the performance of transmission schemes. From the aspect of transmission schemes, we use $\mathrm{NCS_k}$ and $\mathrm{NCS_f}$ to indicate the NCS schemes that are deployed by k-means and fixed-point respectively. It can be seen that the average SE of $\mathrm{NCS_k}$ and $\mathrm{NCS_f}$ are very close, which means that both distance based and the rate based deployment scheme give us similar performance in a LoS dominant environment without CS. However, if PCS is considered in the data transmission with fixed-point deployment scheme, the average data rate is almost tripled when compared to the previous two cases. Besides, it is worth noting that k-means is solely depend on the A2G distance and cannot be combined with the proposed the PCS scheme. Moreover, the minimum data rate threshold will affect the performance of CCS. Hence, we set $\mathrm{R_{min}} = 9.6$ Mbits/s (12 bits/s/Hz) based on the average minimum data rate of the first two scenarios for a fair comparison among these 4 cases. Here, the $\mathrm{R_{min}}$ is not obtained from the minimum data value of all setups, it was calculated by collecting the minimum data rate in each setup and the average of these minimum values was taken. Therefore, it is clear to see from Fig. 9(a) that the average SE of PCS is about 3 times as much as that of $\mathrm{NCS_k}$ and $\mathrm{NCS_f}$. Additionally, the average SE of CCS under this $\mathrm{R_{min}}$ condition is close to 1.5 times of PCS, which further improves the SE of GUs. Furthermore, it could be found from Fig. 9(b) that the increase of threshold $\mathrm{R_{min}}$ will gradually reduce the average SE of CCS, which means that the system cannot exploit more subcarrier resources from those GUs with low-frequency requested contents when their data rate demand is higher. In other words, the optimization need to increase the weight of those low-frequency requested contents in subcarriers to achieve the minimum SE set by $\mathrm{R_{min}}$. Consequently, this will conversely reduce the weight of those high-frequency requested contents since the sum of weight is always fixed to 1.

In the above discussion, we have analyzed the SE of our proposed transmission schemes in LoS dominant scenario.

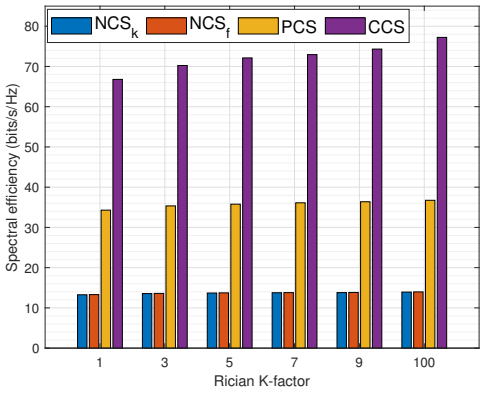

Fig. 10: Illustration of how the K-factor affects the performance of different transmission schemes with $\mathrm{R_{min}}$ = 1 Mbits/s.

However, it is highly possible that the environment is not LoS dominant in some cases. Therefore, Fig. 10 illustrates how the Rician K-factor affects the performance of different transmissin schemes. The x-axis in Fig. 10 shows the Rician K-factor, where the value 100 is presented to show a LoS dominant environment. Also, the threshold $\mathrm{R_{min}}$ is set to 1 Mbits/s. Firstly, it can be found from Fig. 10 that the performance of all these four transmission schemes will be improved with the increase of the K-factor, since the data rate is more related to the A2G distances or h_{LoS}. However, it can also be argued that $\mathrm{NCS_k}$, $\mathrm{NCS_f}$ and PCS are slightly affected by the K-factor compared to the CCS. This phenomenon is closely related to the optimization process of CCS. As mentioned before, the final deployment location is based on the outputs of the optimization at different locations by considering a LoS dominant environment. Hence, if the environment is not LoS dominant, the deployment could mismatch the real channel condition, which will cause a degradation in the performance. In other words, the deployment of CCS in an environment with NLoS component cannot guarantee that the deployment location found by traverse-search is the place where the highest data rate can be achieved. This is also the cause for the other three cases, but it affects more on CCS due to the optimization process conducted in the CCS case.

V. Conclusion

In this work, we proposed two CS transmission schemes, namely PCS and CCS, for UAV-assisted wireless communication by utilizing the content awareness, which aims to increase the SE of GUs. Based on the proposed PCS and CCS schemes, we designed two UAV deployment techniques to find the appropriate UAV position that maximizes the average data rate of the GUs. Our results show that our proposed PCS and CCS transmission schemes as well as their corresponding deployment strategies can significantly improve the average data rate. The simulation results prove that our proposed two CS transmission schemes outperform the traditional transmission scheme by 26 bits/s/Hz and 51 bits/s/Hz, for the PCS and CCS, respectively."

References

[1] Y. Fu, L. Salaün, X. Yang, W. Wen, and T. Q. Quek, "Caching efficiency maximization for device-to-device communication networks: A recommend to cache approach," *IEEE Transactions on Wireless Communications*, vol. 20, no. 10, pp. 6580–6594, 2021.

[2] J. Yao, T. Han, and N. Ansari, "On mobile edge caching," *IEEE Communications Surveys & Tutorials*, vol. 21, no. 3, pp. 2525–2553, 2019.

[3] K. Zhang, S. Leng, Y. He, S. Maharjan, and Y. Zhang, "Cooperative content caching in 5G networks with mobile edge computing," *IEEE Wireless Communications*, vol. 25, no. 3, pp. 80–87, 2018.

[4] M. A. Khan, E. Baccour, Z. Chkirbene, A. Erbad, R. Hamila, M. Hamdi, and M. Gabbouj, "A survey on mobile edge computing for video streaming: Opportunities and challenges," *IEEE Access*, 2022.

[5] G. S. Paschos, G. Iosifidis, M. Tao, D. Towsley, and G. Caire, "The role of caching in future communication systems and networks," *IEEE Journal on Selected Areas in Communications*, vol. 36, no. 6, pp. 1111–1125, 2018.

[6] G. Paschos, E. Bastug, I. Land, G. Caire, and M. Debbah, "Wireless caching: Technical misconceptions and business barriers," *IEEE Communications Magazine*, vol. 54, no. 8, pp. 16–22, 2016.

[7] J. Wang, M. Cheng, K. Wan, and G. Caire, "A Novel Framework for Coded Caching via Cartesian Product with Reduced Subpacketization," in *2022 IEEE International Symposium on Information Theory (ISIT)*. IEEE, 2022, pp. 1300–1305.

[8] R. Bajpai, S. Chakraborty, and N. Gupta, "Adapting Deep Learning for Content Caching Frameworks in Device-to-Device Environments," *IEEE Open Journal of the Communications Society*, 2022.

[9] Y. Zeng and R. Zhang, "Energy-efficient UAV communication with trajectory optimization," *IEEE Transactions on Wireless Communications*, vol. 16, no. 6, pp. 3747–3760, 2017.

[10] R. Shahzadi, M. Ali, H. Z. Khan, and M. Naeem, "UAV assisted 5G and beyond wireless networks: A survey," *Journal of Network and Computer Applications*, vol. 189, p. 103114, 2021.

[11] A. Bürkle, F. Segor, and M. Kollmann, "Towards autonomous micro uav swarms," *Journal of intelligent & robotic systems*, vol. 61, no. 1, pp. 339–353, 2011.

[12] P. McEnroe, S. Wang, and M. Liyanage, "A survey on the convergence of edge computing and AI for UAVs: Opportunities and challenges," *IEEE Internet of Things Journal*, 2022.

[13] M. Ghamari, P. Rangel, M. Mehrubeoglu, G. Tewolde, and R. S. Sherratt, "Unmanned aerial vehicle communications for civil applications: a review," *IEEE Access*, 2022.

[14] B. Alzahrani, O. S. Oubbati, A. Barnawi, M. Atiquzzaman, and D. Alghazzawi, "UAV assistance paradigm: State-of-the-art in applications and challenges," *Journal of Network and Computer Applications*, vol. 166, p. 102706, 2020.

[15] M. Dai, Z. Su, Q. Xu, and N. Zhang, "Vehicle assisted computing offloading for unmanned aerial vehicles in smart city," *IEEE Transactions on Intelligent Transportation Systems*, vol. 22, no. 3, pp. 1932–1944, 2021.

[16] Z. Ning, P. Dong, M. Wen, X. Wang, L. Guo, R. Y. Kwok, and H. V. Poor, "5G-enabled UAV-to-community offloading: joint trajectory design and task scheduling," *IEEE Journal on Selected Areas in Communications*, vol. 39, no. 11, pp. 3306–3320, 2021.

[17] T. Do-Duy, L. D. Nguyen, T. Q. Duong, S. R. Khosravirad, and H. Claussen, "Joint optimisation of real-time deployment and resource allocation for UAV-aided disaster emergency communications," *IEEE Journal on Selected Areas in Communications*, vol. 39, no. 11, pp. 3411–3424, 2021.

[18] D.-H. Tran, V.-D. Nguyen, S. Chatzinotas, T. X. Vu, and B. Ottersten, "UAV relay-assisted emergency communications in IoT networks: Resource allocation and trajectory optimization," *IEEE Transactions on Wireless Communications*, 2021.

[19] M. Mozaffari, W. Saad, M. Bennis, Y.-H. Nam, and M. Debbah, "A tutorial on UAVs for wireless networks: Applications, challenges, and open problems," *IEEE communications surveys & tutorials*, vol. 21, no. 3, pp. 2334–2360, 2019.

[20] H. Nawaz, H. M. Ali, and A. A. Laghari, "UAV communication networks issues: a review," *Archives of Computational Methods in Engineering*, vol. 28, no. 3, pp. 1349–1369, 2021.

[21] S. H. Alsamhi, A. V. Shvetsov, S. Kumar, J. Hassan, M. A. Alhartomi, S. V. Shvetsova, R. Sahal, and A. Hawbani, "Computing in the sky: A survey on intelligent ubiquitous computing for uav-assisted 6g networks and industry 4.0/5.0," *Drones*, vol. 6, no. 7, p. 177, 2022.

[22] J. Ni, K. Zhang, and A. V. Vasilakos, "Security and privacy for mobile edge caching: Challenges and solutions," *IEEE Wireless Communications*, vol. 28, no. 3, pp. 77–83, 2020.

[23] M. Zhang, M. El-Hajjar, and S. X. Ng, "Intelligent Caching in UAV-Aided Networks," *IEEE Transactions on Vehicular Technology*, 2021.

[24] Z. Lin, M. Lin, T. De Cola, J.-B. Wang, W.-P. Zhu, and J. Cheng, "Supporting IoT with rate-splitting multiple access in satellite and aerial-integrated networks," *IEEE Internet of Things Journal*, vol. 8, no. 14, pp. 11 123–11 134, 2021.

[25] E. Danish, V. De Silva, A. Fernando, C. De Alwis, and A. Kondoz, "Content-aware resource allocation in OFDM systems for energy-efficient video transmission," *IEEE Transactions on Consumer Electronics*, vol. 60, no. 3, pp. 320–328, 2014.

[26] H. Wu, N. Zhang, Z. Wei, S. Zhang, X. Tao, X. Shen, and P. Zhang, "Content-aware cooperative transmission in HetNets with consideration of base station height," *IEEE Transactions on Vehicular Technology*, vol. 67, no. 7, pp. 6048–6062, 2018.

[27] S. Baidya, Y. Chen, and M. Levorato, "eBPF-based content and computation-aware communication for real-time edge computing," in *IEEE INFOCOM 2018-IEEE Conference on Computer Communications Workshops (INFOCOM WKSHPS)*. IEEE, 2018, pp. 865–870.

[28] P. Dinh, T. M. Nguyen, C. Assi, and W. Ajib, "Joint beamforming and location optimization for cooperative content-aware UAVs," in *2019 IEEE Wireless Communications and Networking Conference (WCNC)*. IEEE, 2019, pp. 1–7.

[29] P. Dinh, T. M. Nguyen, S. Sharafeddine, and C. Assi, "Joint location and beamforming design for cooperative UAVs with limited storage capacity," *IEEE Transactions on Communications*, vol. 67, no. 11, pp. 8112–8123, 2019.

[30] L. Sun, D. Huang, and A. L. Swindlehurst, "Fountain-coding aided secure transmission with delay and content awareness," *IEEE Transactions on Vehicular Technology*, vol. 69, no. 7, pp. 7992–7997, 2020.

[31] A. M. Alenezi and K. A. Hamdi, "Reinforcement Learning Approach for Content-Aware Resource Allocation in Hybrid WiFi-VLC Networks," in *2021 IEEE 93rd Vehicular Technology Conference (VTC2021-Spring)*. IEEE, 2021, pp. 1–5.

[32] Z. Yang, M. Chen, W. Saad, and M. Shikh-Bahaei, "Optimization of rate allocation and power control for rate splitting multiple access (RSMA)," *IEEE Transactions on Communications*, vol. 69, no. 9, pp. 5988–6002, 2021.

[33] Y. Mao, O. Dizdar, B. Clerckx, R. Schober, P. Popovski, and H. V. Poor, "Rate-splitting multiple access: Fundamentals, survey, and future research trends," *IEEE Communications Surveys & Tutorials*, 2022.

[34] N. Jindal and A. Goldsmith, "Optimal power allocation for parallel gaussian broadcast channels with independent and common information," in *Int. Symp. Information Theory, Chicago, IL*, 2004.

[35] M. Dai, B. Clerckx, D. Gesbert, and G. Caire, "A rate splitting strategy for massive MIMO with imperfect CSIT," *IEEE Transactions on Wireless Communications*, vol. 15, no. 7, pp. 4611–4624, 2016.

[36] O. Dizdar, Y. Mao, W. Han, and B. Clerckx, "Rate-splitting multiple access: A new frontier for the PHY layer of 6G," in *2020 IEEE 92nd Vehicular Technology Conference (VTC2020-Fall)*. IEEE, 2020, pp. 1–7.

[37] H. Holma and A. Toskala, *LTE for UMTS: OFDMA and SC-FDMA based radio access*. John Wiley & Sons, 2009.

[38] I. Al-Surmi, A. M. Mansoor, and A. A. Ahmed, "Toward 5G high utilizations: a survey on OFDMA-based resource allocation techniques in next-generation broadband wireless access networks," *EAI Endorsed Transactions on Mobile Communications and Applications*, vol. 6, no. 18, pp. e3–e3, 2021.

[39] B. Bossy, P. Kryszkiewicz, and H. Bogucka, "Energy-Efficient OFDM Radio Resource Allocation Optimization With Computational Awareness: A Survey," *IEEE Access*, vol. 10, pp. 94 100–94 132, 2022.

[40] L. D. Nguyen, K. K. Nguyen, A. Kortun, and T. Q. Duong, "Real-time deployment and resource allocation for distributed UAV systems in disaster relief," in *2019 IEEE 20th International Workshop on Signal Processing Advances in Wireless Communications (SPAWC)*. IEEE, 2019, pp. 1–5.

[41] I. Valiulahi and C. Masouros, "Multi-UAV deployment for throughput maximization in the presence of co-channel interference," *IEEE Internet of Things Journal*, vol. 8, no. 5, pp. 3605–3618, 2020.

[42] N. Lin, Y. Liu, L. Zhao, D. O. Wu, and Y. Wang, "An Adaptive UAV Deployment Scheme for Emergency Networking," *IEEE Transactions on Wireless Communications*, vol. 21, no. 4, pp. 2383–2398, 2021.

[43] Z. Chen, H. Zheng, J. Zhang, X. Zheng, and C. Rong, "Joint computation offloading and deployment optimization in multi-UAV-enabled MEC systems," *Peer-to-Peer Networking and Applications*, vol. 15, no. 1, pp. 194–205, 2022.

[44] F. Xu, Z. Zhang, J. Feng, Z. Qin, and Y. Xie, "Efficient deployment of multi-UAV assisted mobile edge computing: A cost and energy perspective," *Transactions on Emerging Telecommunications Technologies*, p. e4453, 2022.

[45] Z. Dai, Y. Zhang, W. Zhang, X. Luo, and Z. He, "A Multi-Agent Collaborative Environment Learning Method for UAV Deployment and Resource Allocation," *IEEE Transactions on Signal and Information Processing over Networks*, vol. 8, pp. 120–130, 2022.

[46] A. Granas and J. Dugundji, *Fixed point theory*. Springer Science & Business Media, 2013.

[47] L. Liu, S. Zhang, and R. Zhang, "CoMP in the sky: UAV placement and movement optimization for multi-user communications," *IEEE Transactions on Communications*, vol. 67, no. 8, pp. 5645–5658, 2019.

[48] K. Seong, M. Mohseni, and J. M. Cioffi, "Optimal resource allocation for OFDMA downlink systems," in *2006 IEEE International Symposium on Information Theory*. IEEE, 2006, pp. 1394–1398.

[49] J. Lyu, Y. Zeng, R. Zhang, and T. J. Lim, "Placement optimization of UAV-mounted mobile base stations," *IEEE Communications Letters*, vol. 21, no. 3, pp. 604–607, 2016.

[50] H. Zhang, L. Song, Z. Han, and H. V. Poor, "Cooperation techniques for a cellular internet of unmanned aerial vehicles," *IEEE Wireless Communications*, vol. 26, no. 5, pp. 167–173, 2019.

[51] Y. Liu, K. Xiong, Y. Lu, Q. Ni, P. Fan, and K. B. Letaief, "UAV-Aided Wireless Power Transfer and Data Collection in Rician Fading," *IEEE Journal on Selected Areas in Communications*, vol. 39, no. 10, pp. 3097–3113, 2021.

[52] V. Erceg, P. Soma, D. S. Baum, and A. J. Paulraj, "Capacity obtained from multiple-input multiple-output channel measurements in fixed wireless environments at 2.5 GHz," in *2002 IEEE International Conference on Communications. Conference Proceedings. ICC 2002 (Cat. No. 02CH37333)*, vol. 1. IEEE, 2002, pp. 396–400.

[53] S. Zhu, T. S. Ghazaany, S. M. Jones, R. A. Abd-Alhameed, J. M. Noras, T. Van Buren, J. Wilson, T. Suggett, and S. Marker, "Probability Distribution of Rician K-Factor in Urban, Suburban and Rural Areas Using Real-World Captured Data," *IEEE Transactions on Antennas and Propagation*, vol. 62, no. 7, pp. 3835–3839, 2014.

[54] S. Suman, S. Kumar, and S. De, "Path loss model for UAV-assisted RFET," *IEEE Communications Letters*, vol. 22, no. 10, pp. 2048–2051, 2018.

[55] T. S. Rappaport, "Mobile radio propagation: Large-scale path loss," *Wireless communications: principles and practice*, pp. 107–110, 2002.

[56] B. S. Chaudhari and M. Zennaro, *LPWAN Technologies for IoT and M2M Applications*. Academic Press, 2020.

[57] L. Gupta, R. Jain, and G. Vaszkun, "Survey of important issues in UAV communication networks," *IEEE Communications Surveys & Tutorials*, vol. 18, no. 2, pp. 1123–1152, 2015.

[58] C. E. Shannon, "A mathematical theory of communication," *ACM SIGMOBILE mobile computing and communications review*, vol. 5, no. 1, pp. 3–55, 2001.

[59] R. J. Vanderbei *et al.*, *Linear programming*. Springer, 2020.

[60] Q. Ye, B. Rong, Y. Chen, M. Al-Shalash, C. Caramanis, and J. G. Andrews, "User association for load balancing in heterogeneous cellular networks," *IEEE Transactions on Wireless Communications*, vol. 12, no. 6, pp. 2706–2716, 2013.

[61] D. Liu, L. Wang, Y. Chen, M. Elkashlan, K.-K. Wong, R. Schober, and L. Hanzo, "User association in 5G networks: A survey and an outlook," *IEEE Communications Surveys & Tutorials*, vol. 18, no. 2, pp. 1018–1044, 2016.

[62] L. Liu, W. Hong, H. Wang, G. Yang, N. Zhang, H. Zhao, J. Chang, C. Yu, X. Yu, H. Tang *et al.*, "Characterization of line-of-sight MIMO channel for fixed wireless communications," *IEEE Antennas and Wireless Propagation Letters*, vol. 6, pp. 36–39, 2007.